

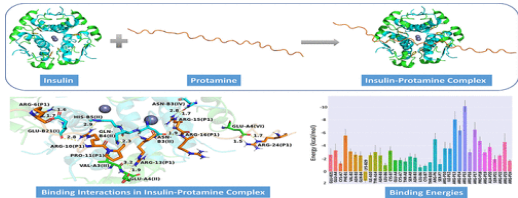
Sl. No.	<p style="text-align: center;">IIT Ropar List of Recent Publications with Abstract Coverage: January, 2024</p>
1.	<p><u>A coil rectenna array design to harvest all H-field components for lateral misalignment tolerant wireless powering of bio-medical implant devices</u> VK Srivastava, A Sharma - IEEE Journal of Electromagnetics, RF and Microwaves in Medicine and Biology, 2024</p> <p>Abstract: This paper presents a coil rectenna array design to address the lateral misalignment problem in near-field wireless powering of biomedical implants and wearable devices. For this purpose, the proposed design comprises three non-identical orthogonal coil antennas optimized to harvest three orthogonal H-field components efficiently. The rectified energy generated by these antenna units is utilized to supply power to the load by combining the individual rectified output voltages. Out of the two distinct combining techniques, DC and AC combining, DC combining proved advantageous in effectively harnessing the lateral field components. The design parameters of the orthogonal coil rectennas are optimized to enhance the lateral misalignment tolerance area. To realize the proposed rectenna array, a multi-layer PCB technology is employed, resulting in a compact, robust, and cost-effective solution for wireless powering of biomedical implanted and wearable devices. Experimental validation of the analytical results demonstrates that the proposed design has the potential to significantly mitigate the lateral misalignment problem in a 2D plane, achieving a uniformity percentage of 38.18 % for a misalignment tolerance range of 60×60 mm².</p>
2.	<p><u>A further study on weak byzantine gathering of mobile agents</u> A Saxena, K Mondal - ICDCN '24: International Conference on Distributed Computing and Networking, 2024</p> <p>Abstract: The gathering of mobile agents in the presence of Byzantine faults is first studied by Dieudonné et al.. Authors provide a polynomial time algorithm handling any number of weak Byzantine agents in the presence of at least one good agent considering start-up delays, i.e., the good agents may not wake up at the same time. Hirose et al. come up with an algorithm considering start-up delays that use a strong team of at least $4f^2 + 8f + 4$ many good agents but runs much faster than that of Dieudonné et al.. Later Hirose et al. provide another polynomial time algorithm for gathering in the presence of at least $8f + 8$ good agents. However, this algorithm does not work in the presence of start-up delays, also simultaneous termination of good agents is not possible. We, in this work, provide an algorithm considering start-up delays of the good agents reducing the number of good agents w.r.t. Hirose et al. from $4f^2 + 8f + 4$ to $f^2 + 4f + 9$. Also, our algorithm guarantees simultaneous termination of the good agents.</p>
3.	<p><u>Alpha clustering in 41, 45, 49Ca* nuclei formed in neutron induced reactions</u> M Kaur, BB Singh, SK Patra, PK Raina - Journal of Physics: Conference Series, 2023</p> <p>Abstract: The light neutron-rich nuclei play a vital role in nucleosynthesis process and the extent of alpha (α) clustering significantly influence the astrophysical rates. Thus, it is significant to explore the α clustering in these nuclei and in the present work, we have studied the α clustering in 41,45,49Ca* nuclei formed in neutron induced reactions within the dynamical cluster decay model (DCM). The results present that with progression towards neutron-rich 45Ca* and 49Ca* nuclei, there is a significant decrease in the α-cluster preformation factor P_0. The inclusion of relativistic mean field theory (RMFT) based microscopic temperature-dependent binding energies (T.B.E.) within DCM, give relatively enhanced α-cluster preformation factor for 41,45,49Ca* nuclei compared to the case of macroscopic T.B.E. based upon Davidson mass formula. The cross-section associated with α-cluster emission depicts strong isospin dependence</p>

	<p>and falls off significantly with increasing neutron number of Ca* nuclei. Further, for the first time, we inculcate the microscopic nuclear potential constructed via folding the standard Fermi form fitted RMFT cluster densities and M3Y nucleon-nucleon interaction within the DCM. The neutron skin thickness of the Ar cluster, complementary to α-cluster, is varied and its effect upon the nuclear interaction potential and α-cluster preformation factor is analysed. The results present that with growing neutron skin of Ar cluster, the α-cluster preformation factor decreases. It explores a strong correlation among the neutron skin thickness and α-cluster preformation factor in light mass 41,45,49Ca* nuclear systems.</p>
4.	<p>Analysis of axisymmetric hollow cylinder under surface loading using variational principle AV Sirsat, SS Padhee - Mathematics and Mechanics of Solids, 2024</p> <p>Abstract: In this work, a variational principle-based approach has been adopted to analyze one of the classical linear elasticity problem of the axisymmetric cylinder under surface loading. The use of variational principle results in a set of governing partial differential equations with associated boundary conditions. The equations have been solved using the separation of variable approach and the Frobenius method. A general solution has been derived and used to solve two test cases. The proposed solution is capable of meeting all the boundary conditions. The solution has been validated by comparing it with a finite element-based numerical solution and considering a special limiting condition of a solid cylinder, for which results are available in the literature. Further various studies have been carried out to understand the robustness and limitation of the presented solution.</p>
5.	<p>Analytic solution to isotropic axisymmetric cylinder under surface loadings problem through variational principle AV Sirsat, SS Padhee - Acta Mechanica, 2024</p> <p>Abstract: Analysis of cylinders under axisymmetric loading is of great interest as it finds many practical application. In this work, an attempt has been made to solve this problem through variational principle. The variational statement results in a set of coupled partial governing equation and associated boundary conditions. The solution has been derived after systematic decoupling of governing equation, application of separation of variables and use of Frobenius method. The resulting solution as demonstrated is capable of satisfying all the boundary conditions in an exact sense. The accuracy and efficiency of the presented solution have been validated for problems available in the literature and against three-dimensional finite element simulations for isotropic homogeneous material. It is observed that the present solution not only has excellent agreement with three-dimensional finite element analysis but also is generic in nature.</p>
6.	<p>Apict: air pollution epidemiology using green AQI prediction during winter seasons in India S Dey, K Chatterjee, RP Kumar...- IEEE Transactions on Sustainable Computing, 2024</p> <p>Abstract: During the winter season in India, the AQI experiences a decrease due to the limited dispersion of APs caused by MFs. Therefore, we developed a sophisticated green predictive model GAP, which utilizes our designed green technique and a customized big dataset. This dataset is derived from weather research and tailored to forecast future AQI levels in the Indian subcontinent during winter. This dataset has been meticulously curated by amalgamating samples of APs and MFs concentrations, further adjusted to reflect the yearly activity data across various Indian states. The dataset reveals an amplified national emissions rate for , , and pollutants, exhibiting an increase of 3.6%, 1.3%, and 2.5% in gigagrams per day. ML/DL regressors are then applied to this dataset, with the most effective ML/DL regressors being selected based on their performance. Our paper encompasses an exhaustive examination of existing literature within the realm of air pollution epidemiology. The evaluation results demonstrate that the prediction accuracy of GAP when utilizing LSTM, CNN, MLP, and RNN achieve accuracies of 98.53%,</p>

	95.9222%, 96.1555%, and 97.344% in predicting the , , and concentrations. In contrast, RF, KNN, and SVR yield lower accuracies of 92.511%, 90.333%, and 93.566% for the same AQIs.
7.	<p>Assessing future changes in daily precipitation tails over India: insights from multimodel assessment of CMIP6 GCMs N Gupta, SR Chavan - Theoretical and Applied Climatology, 2024</p> <p>Abstract: The tails of the probability distribution host extremes. The distributions are typically classified into heavy or light-tailed distributions subjected to their tail behavior, out of which the former signifies frequent happenings of extreme events. The present study demonstrates the analysis where the outputs from 13 climate models from the Coupled Model Intercomparison Project Phase 6 (CMIP6) are used to evaluate changes in the tail behavior of precipitation extremes that will preside over India for the twenty-first century. A straightforward empirical index known as the “obesity index” (OB) is utilized to measure the tail heaviness for each of the 4801 daily precipitation records over India for historical (1970–2019) and future (2020–2100) time periods. The same approach was used to characterize daily precipitation tails in the Indian meteorological subdivisions and across different climate types during various periods. The results highlight that heavy-tailed distributions are well-suited for daily precipitation extremes in India, with OB values above 0.75 observed in nearly all grids for both present and future scenarios. Notably, in the case of the shared socioeconomic pathway (SSP) 585 climate scenario, which is the worst climate scenario, approximately 42.82% of grids exhibit the highest range of OB from 0.85 to 0.9 relative to other SSP scenarios. The findings also show that the largest to smallest heavy tails are associated with major climate types E (polar), B (arid), A (tropical), and C (temperate). Large heavy-tailed extremes are observed in ET, BSh, BWh, and Aw for climate subtypes, while relatively lighter-tailed extremes were observed in Am and Cwb. Furthermore, the variation in the OB is found to be non-linear with the elevation. In climatic zones Aw, BSh, Cwa, and ET, a U-shaped pattern is observed, while in climate zone Cwb, it shows a concave increase. Conversely, curves are convex decreasing for As, BWh, Csa, and convex increasing for zone Am. The conclusions from this study can help policymakers in designing adaptation plans in response to the anticipated effects of climate change.</p>
8.	<p>Assessment of natural radioactivity in soil around Khetri copper belt of Rajasthan, India N Kumar, B Khyalia...PP Singh... - Journal of Radioanalytical and Nuclear Chemistry, 2024</p> <p>Abstract: The concentration of natural radionuclides (^{226}Ra, ^{232}Th, ^{40}K) in the fifty soil samples around the Khetri copper belt is measured using an HPGe detector. The values of ^{226}Ra, ^{232}Th, and ^{40}K are found to be lying in the range of 5.2 ± 0.3 to $27.5 \pm 0.6 \text{ Bq kg}^{-1}$, 12.9 ± 0.4 to $38.8 \pm 1.3 \text{ Bq kg}^{-1}$, and 113.3 ± 27.8 to $308.5 \pm 31.2 \text{ Bq kg}^{-1}$ respectively. The radium equivalent activity ranged from 38.63 to 93.35 Bq kg^{-1} with a mean value of 56.21 Bq kg^{-1}. The values of absorbed dose rate, annual effective dose, and annual gonadal dose rate are also estimated, which comes out to be less than their corresponding world average values. Hazard indices (internal and external) and level indices (alpha and gamma) are also observed to be less than unity. The soil of the study area can be considered safe for people living there because of its low radiological risk.</p>
9.	<p>Autofocusing and self-healing of partially blocked circular Airy derivative beams A Kumari, V Dev, V Pal - Optics & Laser Technology, 2024</p> <p>Abstract: We numerically and experimentally study the autofocusing and self-healing of partially blocked circular Airy derivative beams (CADBs). The CADB consists of multiple rings, and partial blocking of CADB with different kinds is achieved by using symmetric and asymmetric binary amplitude apertures, enabling blocking of inner/outer rings and sectorially. The CADB blocked with different types possesses the ability to <u>autofocus</u>, however, the abruptness in the autofocusing varies with the amount in certain types of blocking. The abrupt autofocusing is quantified by a maximum k-value, and how fast it changes around the</p>

	<p>autofocusing distance (z_{af}). In particular, CADB blocked with inner rings (first/two/three) exhibits an abrupt autofocusing, as the k-value sharply increases [decreases] just before [after] z_{af}. The maximum k-value always occurs at z_{af}, which decreases as the number of blocked inner rings increases. For CADB blocked with outer rings, the k-value gradually changes around z_{af}, indicating a lack of abrupt autofocusing. The value of z_{af} increases with the number of blocked outer rings. This suggests that although outer rings contain low intensities, these play an important role in abrupt autofocusing. A sectorially blocked CADB possesses an abrupt autofocusing, and maximum k-value depends on the amount of blocking. The CADB blocked with different types possesses good self-healing abilities, where blocked parts reappear as a result of redistribution of intensity. The maximum self-healing occurs at z_{af}, where an overlap integral approaches a maximum value. Finally, we have compared ideal CADB and partially blocked CADB having the same radii of central dark region, and found that an ideal CADB possesses better abrupt autofocusing. We have found a good agreement between the numerical simulations and experimental results.</p>
10.	<p>Biogenic nanomaterials for chemosensor applications A Sharma, G Singh, N Singh, N Kaur - Biogenic Nanomaterial for Health and Environment: Book Chapter, 2023</p> <p>Abstract: Replacing petroleum-based chemicals/products and utilization of biomass or waste valorization are among the long pursuits of scientific research to attain a sustainable circular bioeconomy. For chemosensor applications, biogenic nanomaterials have significant benefits over conventionally manufactured nanomaterials. Researchers are continuously investigating strategies to control the morphology of biogenic nanostructure manufacturing as well as new biogenic nanomaterials and their use for diverse sensing applications. This chapter includes both charged and uncharged species, which are mainly of utmost environmental concern, and discussion about the various types of biomass sources that can be used to prepare luminescent materials, their structure-optical performance correlation, preparation methods, optical properties, potential applications, as well as future challenges and perspectives.</p>
11.	<p>Biomedical applications of biogenic carbon-based fluorescent nanoparticles K Kaur, G Singh, R Badru, N Kaur, N Singh - Biogenic Nanomaterial for Health and Environment: Book Chapter, 2023</p> <p>Abstract: The wide-ranging applications of carbon dots (CDs), which can be developed using either green or chemical precursors, have been made possible due to their reported properties and the various precursors that have been identified. This has opened up new opportunities for the development of high-quality CDs and their use in optoelectronic devices, bioimaging, and other applications. Green precursors can be derived from fruits, vegetables, flowers, leaves, seeds, stems, crop residues, fungi/bacteria species, and waste products, while chemical precursors can be categorized as either acid reagents or non-acid reagents. It provides a brief review of the past ten years of CD synthesis using both green and chemical precursors, as well as the use of CDs as sensing materials in biomedical applications. This comprehensive review will be a valuable resource for researchers who are interested in synthesizing high-quality CDs for a variety of applications.</p>
12.	<p>Circuit implementation of on-chip trainable spiking neural network using CMOS based memristive STDP synapses and LIF neurons SK Vohra, SA Thomas, M Sakare, DM Das - Integration, 2024</p> <p>Abstract: Computation on a large volume of data at high speed and low power requires energy-efficient architectures for edge computing applications. As a result, scientists focus on memristive circuits and systems for area and energy efficiency. Spiking neural network (SNN)</p>

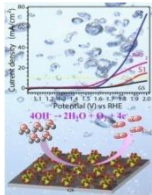
	<p>with bio-inspired spike-timing-dependent plasticity learning (STDP) is a promising solution for energy-efficient neuromorphic systems than conventional artificial neural network (ANN). Previous works on SNN with STDP learning primarily use memristor macro models, which are software-based and cannot give complete insight into circuit implementation challenges. Some reported works on SNN use memristive devices, which require additional fabrication steps. This article presents a full circuit-level implementation of the SNN system featuring on-chip training and classification using memristive STDP synapse in standard CMOS technology. A new learning rule using the modified STDP is implemented to simplify the weight modification process. It does not involve FPGAs, CPUs, or GPUs to train the neural network. The approach used in this paper to modify the weights does not require any additional combinational or digital circuits attached to the memristive synapse resulting in less consumption of area, energy and time. We demonstrated the complete circuit-level design, implementation and simulation of SNN with on-chip training and pattern classification using 180 nm CMOS technology. A comprehensive comparison of the proposed SNN circuit with the previous related work is also presented. To demonstrate the versatility of the CMOS synapse circuit for application scenarios requiring rate-based learning, we have tuned the pair-based STDP circuit to obtain Bienenstock–Cooper–Munro (BCM) characteristics and applied it to heart rate classification.</p>
13.	<p>Colorimetric nanozyme sensor array based on metal nanoparticle-decorated CNTs for quantification of pesticides in real water and soil samples M Kumar, N Kaur, N Singh - ACS Sustainable Chemistry & Engineering, 2024</p> <p>Abstract: Pesticides have become a concern to the environment and human health, since they are frequently employed to control pests and regulate plant growth. Although array-based pattern recognition has been demonstrated to be a successful method for identifying a variety of analytes, developing sensing components that possess a desirable surface diversity remains a difficult task. Herein, we fabricated a metal nanoparticle-decorated CNT (MDC) nanozyme in the presence of a cationic receptor to produce diverse noncovalent interactions when various pesticides were adsorbed on the MDCs, which resulted in the enhancement of their peroxidase-mimicking activities with different degrees, and utilized it as a colorimetric sensor array for pesticide identification. The designed MDC sensor array could successfully distinguish eight pesticides that exhibited different fingerprint-like sequences at a concentration of 10 μM or successfully segregated CBZ, DTM, and ISP pesticides having a linear range varying from 1 to 8 μM and quantified as low as 10.8, 28.8, and 16.8 nM with R^2 values of 0.983, 0.949, and 0.977, respectively. Very interestingly, two pesticides having similar structures (CBZ and ISP) have been precisely discriminated by a sensor array without any overlapping. Additionally, the effective segregation of pesticides in spiked soil and water samples without cross-classification demonstrated the practicability of the MDC sensor array.</p>
14.	<p>Comparative analysis of single-crater parameters in ultrasonic-assisted and unassisted micro-EDM of Ti6Al4V using discharge plasma imaging S Raza, C Nirala - Nanotechnology and Precision Engineering, 2024</p> <p>Abstract: Ultrasonic-assisted micro-electro-discharge machining (μEDM) has the potential to enhance processing responses such as material removal rate (MRR) and surface finish. To understand the reasons for this enhancement, the physical mechanisms responsible for the individual discharges and the craters that they form need to be explored. This work examines features of craters formed by single discharges at various parameter values in both conventional and ultrasonic-assisted μEDM of Ti6Al4V. High-speed imaging of the plasma channel is performed, and data on the individual discharges are captured in real-time. A 2D axisymmetric model using finite element software is established to model crater formation. On the basis of simulation and experimental results, a comparative study is then carried out to examine the effects of ultrasonic vibrational assistance on crater geometry. For every set of μEDM parameters, the crater diameter and depth from a single discharge are found to be higher in</p>

	ultrasonic-assisted μ EDM than in conventional μ EDM. The improved crater geometry and the reduced bulge formation at the crater edges are attributed to the increased melt pool velocity and temperature predicted by the model.
15.	<p>Computational approach to elucidating insulin–protamine binding interactions and dynamics in insulin NPH formulations KK Rohilla, MK Pandey - ACS Omega, 2024</p> <p>Abstract: Insulin NPH is an intermediate-acting insulin. Its protracted action profile is due to the formation of microcrystalline suspensions when insulin is complexed with a basic peptide protamine, zinc ion, and phenolic ligands. Despite advancements in analytical techniques, the binding epitope and binding mode of the protamine in the insulin–protamine complex are still unknown. In this study, we used bioinformatics tools such as molecular docking and molecular dynamics (MD) simulations to compute the binding sites and energetics of the insulin–protamine complex. We have taken four naturally occurring protamine peptides that are independently docked with the insulin R6 hexamer and subjected them to 200 ns MD simulations to observe the dynamics of the complexes and estimate the binding energies. The arginine-rich protamine peptides were found to bind on the surface of the insulin hexamer through hydrogen bonding, hydrophobic, and electrostatic interactions well supported by the calculated negative binding energies. The overall structure of the insulin hexamer was retained upon binding, highlighting its dynamic stability in the complex. Furthermore, the residues at the termini of the protamine peptides in the complex were seen to be highly dynamic, which stabilize toward the end of the simulation.</p> 
16.	<p>Detection of type-II diabetes using graphene-based biosensors B Roondhe, S Saha, W Luo, R Ahuja, S Saxena - Journal of Physics D: Applied Physics, 2024</p> <p>Abstract: Diabetes is a global pandemic that increases the risk of various health complications, including heart attacks, renal failure, blindness, stroke, and peripheral neuropathy. Type-2 Diabetes (T2D) results from an imbalance in lipid and glucose metabolism due to hostility to insulin action and insufficient insulin production response. Valine amino acid has been identified as a potential biomarker for T2D, but there have been no rigorous studies on its interaction with branch chain amino acids. In this study, we investigated the potential of graphene/modified graphene as a valine biosensor using density functional theory to examine the electronic properties and adsorption behavior of graphene, Si-doped graphene, and Pdoped graphene. The adsorption of valine over the substrates was physisorption in nature, and the adsorption energies were in the order of SiG>G>PG. DOS and PDOS calculations confirmed the molecule's adsorption over the monolayers and indicated variations in the electronic properties. We also performed recovery time calculations to examine the reusability of the nano-surfaces as potential biosensors. Ultrafast recovery times were predicted for all three systems, with Si-doped graphene showing the best results. Our study suggests that Si-doped graphene could be used as a biosensor for valine, providing a real-time and efficient diagnostic tool for T2D.</p>
17.	<p>Development of a new instrumented structure for the measurement of avalanche impact pressure RK Aggarwal, R Das, HS Gusain - Fluid Mechanics and Fluid Power (Vol. 7): Select Proceedings of FMFP 2022: Book Chapter, 2024</p> <p>Abstract: Accurate knowledge of avalanche impact pressure is vital for the design of avalanche</p>

	<p>control middle-zone and run-out zone structures. Very little database is available in this regard. With the motivation to fill the knowledge gaps in this area and to develop comprehensive database towards improved guidelines for the avalanche impact pressures on the avalanche control structures, an instrumented structure of size 1.0 m height and 0.65 m width has been developed and installed on a 61 m long experimental facility snow chute located at Field Research Station, Dhundhi (near Manali, Himachal Pradesh), India, for avalanche impact pressure measurement. Four equally spaced piezoelectric force sensors are fitted in the centre of the structure. The measured data has been analysed and compared with the theoretically estimated avalanche impact pressures acquired using the Voellmy–Salm model, and both are found in reasonably good agreement with each other. The obtained results portray that the maximum avalanche impact pressure varies in the range of approximately 15–40 kPa, and the present theoretical predictions are accurate within 20.4% with respect to the experimental observations.</p>
18.	<p>Distance-2-dispersion with termination by a strong team B Gorain, T Kaur, K Mondal - Conference on Algorithms and Discrete Applied Mathematics, 2024</p> <p>Abstract: Distance-2-Dispersion (D-2-D) problem aims to disperse k mobile robots starting from an arbitrary initial configuration on an anonymous port-labeled graph G with n nodes such that no two robots occupy adjacent nodes in the final configuration, though multiple robots may occupy a single node if there is no other empty node whose all adjacent nodes are also empty. In the existing literature, this problem is solved starting from a rooted configuration for robots using synchronous rounds with a total of memory per robot, where m is the number of edges and is the maximum degree of the graph. In this work, we start with mobile robots and improve the run time to $O(m)$ starting from a rooted configuration using the same amount of memory per robot. Further, we achieve D-2-D for an arbitrary initial configuration in $O(pm)$ rounds using memory per robot, where p is the number of nodes containing robots in the initial configuration. Both the algorithms terminate without any global knowledge of . As we start with robots, the nodes occupied by robots in the final configuration form a maximal independent set of the graph.</p>
19.	<p>Do nanobubbles exist in pure alcohol? H Sharma, M Trivedi, N Nirmalkar - Langmuir, 2024</p> <p>Abstract: The existence of nanobubbles in pure water has been extensively debated in recent years, and it is speculated that nanobubbles may be ion-stabilized. However, nanobubbles in the alcohol-water mixture and pure alcohols are still controversial due to the lack of ions present in the alcohol system. This work tested the hypothesis that stable nanobubbles exist in pure alcohol. The ultrasound and oscillatory pressure fields are used to generate nanobubbles in pure alcohol. The size distribution, concentration, diameter, and scattering intensity of the nanobubbles were measured by nanoparticle tracking analysis. The light scattering method measures the zeta potential. The Mie scattering theory and electromagnetic wave simulation are utilized to estimate the refractive index (RI) of nanobubbles from the experimentally measured scattering light intensity. The average RI of the nanobubbles in pure alcohols produced by ultrasound and oscillating pressure fields was estimated to be 1.17 ± 0.03. Degassing the nanobubble sample reduces its concentration and increases its size. The average zeta potential of the nanobubbles in pure alcohol was measured to be -5 ± 0.9 mV. The mechanical stability model, which depends on force balance around a single nanobubble, also predicts the presence of nanobubbles in pure alcohol. The nanobubbles in higher-order alcohols were found to be marginally colloidally stable. In summary, both experimental and theoretical results suggest the existence of nanobubbles in pure alcohol.</p>
20.	<p>EdgeMatch: a smart approach for scheduling IoT-edge tasks with multiple criteria using game theory</p>

	<p>A Bandopadhyay, V Mishra, S Swain, K Chatterjee, S Dey... - IEEE Access, 2024</p> <p>Abstract: For an extended period, a technological architecture known as cloud IoT links IoT devices to servers located in cloud data centers. Real-time data analytic are made possible by this, enabling better, data-driven decision making, optimization, and risk reduction. Since cloud systems are often located at a considerable distance from IoT devices, the rise of time-sensitive IoT applications has driven the requirement to extend cloud architecture for timely delivery of critical services. Balancing the allocation of IoT services to appropriate edge nodes while guaranteeing low latency and efficient resource utilization remains a challenging task. Since edge nodes have lower resource capabilities than the cloud. The primary drawback of current methods in this situation is that they only tackle the scheduling issue from one side. Task scheduling plays a pivotal role in various domains, including cloud computing, operating systems, and parallel processing, enabling effective management of computational resources. In this research, we provide a multiple-factor autonomous IoT-Edge scheduling method based on game theory to solve this issue. Our strategy involves two distinct scenarios. In the first scenario, we introduced an algorithm containing choices for the IoT and edge nodes, allowing them to evaluate each other using factors such as delay and resource usage. The second scenario involves both a centralized and a distributed scheduling approach, leveraging the matching concept and considering each other. In addition, we also introduced a preference-based stable mechanism (PBSM) algorithm for resource allocation. In terms of the execution time for IoT services and the effectiveness of resource consolidation for edge nodes, the technique we use achieves better results compared with the two commonly used Min-Min and Max-Min scheduling algorithms.</p>
21.	<p>Effect of fluid elasticity and shear thinning on heat transfer from a heated sphere at moderate Reynolds numbers</p> <p>A Chauhan, C Sasmal, RP Chhabra - Numerical Heat Transfer, Part A: Applications, 2024</p> <p>Abstract: The drag and heat transfer characteristics of an isothermal sphere in a FENE-P-type viscoelastic fluid have been studied in the steady axisymmetric flow regime. The governing equations, namely, mass, momentum, and energy equations, together with FENE-P type viscoelastic constitutive equations, have been solved using the finite volume method based opensource CFD code OpenFOAM over the following ranges of conditions: Reynolds number, (Formula presented.) Prandtl number, (Formula presented.) Weissenberg number, (Formula presented.) and polymer extensibility parameter, (Formula presented.) for a fixed value of the polymer viscosity ratio of (Formula presented.) At low Reynolds numbers, fluid viscoelasticity causes an upward and downward shifting in the axial velocity profiles with reference to that in a Newtonian fluid along the upstream and downstream axis of the sphere, respectively. However, such a shift progressively diminishes with the increasing Reynolds number. Furthermore, a “velocity overshoot” and/or a “negative wake” is also observed in a viscoelastic polymer solution at low Reynolds numbers, and this is accentuated with the increasing Weissenberg number. The separation of boundary layers is seen to be suppressed with the increasing Weissenberg number. The drag coefficient decreases with the Reynolds number irrespective of the fluid type and the corresponding dependence on the Weissenberg number is found to be non-monotonic depending upon the values of Re and L^2. The average Nusselt number always increases with the increasing values of Re, Pr, and Wi and with the decreasing value of L^2. A limited number of simulations have also been carried out to show the effect of the temperature-dependent viscosity of the fluid on the flow dynamics and heat transfer characteristics. Finally, simple correlations for the drag coefficient and average Nusselt number are presented which not only capture the functional dependence but also can be used for the interpolation of the present results for the intermediate values of the governing parameters in a new application.</p>
22.	<p>Effect of interfacial bonding characteristics of flexural fractured pineapple leaf fibre reinforced composites</p> <p>A Ajithram, J. T. W Jappes, A. Desai, R Das, K. R. Sumesh - Interfacial Bonding Characteristics</p>

	<p>in Natural Fiber Reinforced Polymer Composites, 2024</p> <p>Abstract: It is the aim of this piece of research to investigate Pineapple fiber reinforced composites based on natural fibers that are both eco-friendly and possess unique properties, and to take into account their various properties and their eco-friendliness. As a result of their strength, lightness, and affordability, pineapple fibre materials are considered to be stronger, lighter, and more affordable than traditional materials due to the fact that they are stronger, lighter, and more affordable than natural materials. It has been an important research subject for scientists in recent years to investigate the use of natural fibres as reinforcement materials for polymeric composites that can be used in technical applications. There are many advantages of natural fibers, such as continuous supply, easy handling, and a biodegradable nature, which make them a good choice when it comes to textiles. Due to its low cost, low density, hardness, better tolerance for harsh weather conditions, and good performance thermally and mechanically, natural fibres have gained a great deal of popularity worldwide because of their low cost, low density, hardness, and environmental friendliness. A large number of crops are produced every year around the world, and most of the waste produced by these crops does not have any use whatsoever. It is estimated that thousands of tons of different crops are produced every year. As it is well known, agricultural wastes include leaves from pineapples, dates seeds, and shells from various types of dry fruits, as well as other organic wastes. As part of this project, we have combined the wastes from pineapple leaves (PALF) into a single product. There are numerous promising applications for metal, such as the use of metal as an alternative to the construction of automobile bodies in the future, which are currently being investigated.</p>
23.	<p>Effect of seismic design provisions of Indian standards on seismic response of URM infilled RC buildings on hill Z Naorem, P Haldar - Journal of Vibration Engineering & Technologies, 2024</p> <p>Abstract: Purpose: The scarcity of flat lands in the hilly region forces the construction of buildings on sloping terrain with foundations constructed at different levels. These buildings are inherently vulnerable to earthquakes due to horizontal and vertical irregularities that are extremely hard to avoid because of the nature of the terrain. Compounding on that fact, a large stock of buildings in the hilly region have been constructed without following the earthquake-resistant design provisions, the consequences of which were evident in past seismic events such as the 2011 Sikkim earthquake and the 2015 Nepal earthquake. Methods: The paper aims to assess the explicit and combined effect of seismic design provisions of Indian Standards on the seismic response of a set of Un-Reinforced Masonry (URM) infilled Reinforced Concrete (RC) buildings on a hill with the prevalent configuration observed. 3D analytical models have been considered for the RC frame elements with infill-frame interaction taken into account by diagonal strut elements. Incremental dynamic analyses have been performed for a realistic assessment of key parameters influencing the seismic performance of such buildings. Results: It has been observed that the seismic response parameters in terms of joint displacement and inter-storey drift ratio are higher for buildings designed considering only gravity loads as compared to buildings designed as Special Moment Resisting Frame (SMRF) as per relevant Indian seismic design standards whereas minor variations were observed in the roof acceleration and Peak Storey Acceleration (PSA). It has also been observed that collapse probability at any given seismic hazard level reduces significantly when the Gravity Load Designed (GLD) RC building is designed and detailed as SMRF. It has further been observed that the collapse probability of the GLD RC building can be reduced by more than 40% at the design seismic hazard level if seismic design and ductile detailing provisions are implemented.</p>
24.	<p>Electrochemical oxygen generation from VO2 nanoflakes decorated onto graphite sheet ABS Usmani, S Rana... H Sammi, N Sardana... - Journal of Alloys and Compounds, 2024</p>

	<p>Abstract: The present study deals with the synthesis of VO₂ anchored across graphite sheets using a carbothermal reduction technique. The phase identification, elemental, and morphology of the obtained VO₂/graphite <u>heterostructure</u> were examined using analytical techniques. Morphological characterization by FESEM confirms the formation of nanoflakes like the structure of VO₂/graphite heterostructure. The sample obtained was drop cast onto graphite and the material was utilized as a working electrode for the electrochemical oxygen evolution reaction (OER). The VO₂/graphite heterostructure shows an overpotential of 470 mV as compared to V₂O₅/graphite, which has an overpotential of 800 mV during OER in alkaline media. Additionally, the VO₂/graphite <u>electrocatalyst</u> exhibits a low charge transfer resistance of 29.5 Ω and a low Tafel slope value corresponding to 85 mV dec⁻¹. The results signify that the VO₂/graphite heterostructure has emerged as an efficient catalytic material for OER application. Therefore, the present work focuses on the simpler method for the synthesis of VO₂/graphite heterostructure with long-term performance during O₂ evolution and also renders the potential catalytic applications of vanadium-based <u>metal oxide</u>.</p> 
25.	<p>Emerging functionally graded materials for bio-implant applications—design and manufacturing R Kumar, A Agrawal - Additive Manufacturing of Bio-implants, 2024</p> <p>Abstract: Implants are artificial devices that replace damaged body parts and may promote cell proliferation. The need and demand for implant surgery are increasing due to unhealthy lifestyles, trauma, injuries, etc. The implant with customized design and tailored material properties are important due to issues such as stress-shielding and insensitivity/uneasiness after surgery with the conventional implant. In recent years, research in developing new and innovative materials has gained a lot of momentum due to issues caused by the existing materials. However, Functionally Graded Material (FGM) may be a viable option to resolve the problems caused by traditional or mono-material implants. With the development of CAD tools and Additive Manufacturing (AM) techniques, it has become possible to design and fabricate customized implants. FGMs has the potential to mimic the actual architecture of natural bone and organ with their degrees of freedom (i.e., design, material microstructure, and functionality). Such implants are expected to be mechanically stable with moderate strength to eliminate stress-shielding and conducive to tissue growth. This chapter briefly elaborates on the aspect of design, material, and fabrication processes to manufacture customized FGM-based implants.</p>
26.	<p>Environmental sustainability of milk production: a comparative environmental impact analysis and sustainability evaluation AB Singh, P Sarkar, H Singh, G S Dangayach -Frontiers in Sustainability, 2024</p> <p>Abstract: Context: Assessing the sustainability of milk production in India (the largest milk producer country in the world) is essential to ensure that the dairy industry can meet the growing demands for dairy products while minimizing its negative impact on the environment, society, and the well-being of the people involved in the sector. Objective: Current research is intended to compare the emissions associated with packed milk production in two contrasting states, Punjab (an Indian state with helpful agricultural resources and plenty of water) and Rajasthan (a state with a significant desert area) of India. The dairy industry has to undergo different production processes, including livestock, feed, farming, transportation, processing, packaging, and distribution. All of these production steps generate environmental impacts. This study aims to compare the environmental impacts of milk production in Punjab and Rajasthan by</p>

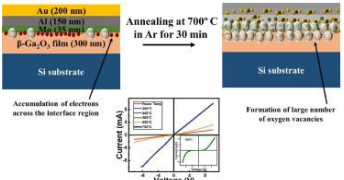
	<p>understanding the variation in the ecological effects due to the modifications adopted in dairy practices. Methods: This study uses Umberto LCA+ with Ecoinvent v3.6 dataset as a Life cycle assessment (LCA) tool and data collected from milk producers and processing plants. The primary data was collected from farmers (milk producers) and dairy plants (processing plants), real-time observations, and inputs from the processing plant staff. The LCA analysis was performed, including parameters such as feed agriculture, milking, storage, transportation, processing, packaging, and distribution. Results and conclusion: The analysis results indicate that milk production in Punjab is more environmentally efficient than in Rajasthan, and the feed required for cattle is a critical environmental impact-generating activity along with the selection of packaging material for processed milk. Significance: The current article assesses the environmental implications of milk production. The study employs a comprehensive analysis to inform sustainable practices and reduce the ecological footprint of this crucial industry.</p>
27.	<p>Estimation of glacial lake dynamics in the Sikkim Himalayas by the inferential statistical techniques D Gaikwad, S Guha, RK Tiwari - Recent Research on Environmental Earth Sciences, Geomorphology, Soil Science, Paleoclimate, and Karst: Proceedings of international conference on Mediterranean Geosciences Union- 2021: Book Chapter, 2023</p> <p>Abstract: Himalayan glaciers are retreating under the climate warming scenario, leading to the temporal variation in the expansion and formation of glacial lakes, which have been identified as highly susceptible to Glacial Lake outburst floods (GLOFs). Therefore, the present study intends to estimate the glacial lake area changes (RGLAC) rate for the entire Sikkim Himalaya by extracting twenty-four samples of glacial lakes using non-parametric inferential statistics. Results showed that the area of sample glacial lakes increased from 9.62 km² to 13.59 km² between 1988 and 2020; overall increased by 41.27%. The highest RGLAC was observed during 2008–2013; after that, it decreased continuously. Furthermore, the maximum volume change among all the large glacial lakes (≥ 1 km²) was observed in GL-18. Hence, this study suggests exploring the dynamics of glacial lakes, especially the larger ones, to make better plans to mitigate the damages and minimize the losses due to GLOFs.</p>
28.	<p>Examining the contribution of tamping effect on inter-splat bonding during cold spray G Vinay, S Halder, R Kant, H Singh - Materials Science and Engineering: A, 2024</p> <p>Abstract: In Cold Spray Additive Manufacturing (CSAM), the 'tamping effect'—resulting from continuous impact of incoming particles enhances the mechanical properties of deposited layers. While the impact of tamping on porosity is well-studied, its influence on inter-splat bonding remains unexplored. In this study a multiparticle simulation based on Finite Element Analysis (FEA) is employed, featuring 120 particles distributed across 12 layers to model the deposition process in cold spray. A methodology is developed to discern the effect of tamping, enabling the estimation of particle boundary temperatures under conditions with and without tamping. Energy analysis and inter-splat boundary temperature variations obtained from simulations are examined to understand the contribution of tamping to bonding. Our findings reveal a significant increase in inter-splat boundary temperatures, attributed to energy transfer from overlying layers, positively impacting bonding. The proposed hypothesis is substantiated through mechanical testing and the assessment of inter-splat bonding-related properties, including hardness, tensile strength, scratch resistance, and corrosion resistance, as a function of deposit thickness. CSAM IN718 and Cu deposits with a thickness of 4 mm are used as subjects for this study.</p>
29.	<p>Flow visualization and parameter suitability in cold spray titanium deposition: A CFD approach P Singh, S Singh, H Singh - Advances in Manufacturing Technology XXXVI: Proceedings of International Conference on Manufacturing Research, ICMR 2022: Book Chapter, 2023</p> <p>Abstract: Cold Spray is an emerging technology in the domain of additive manufacturing. It is a solid-state high strain rate material deposition technique. It uses a supersonic (2–4 Mach) impact</p>

	<p>of process gas (such as nitrogen or helium) to deposit micron-sized (1-100 μm) metallic or composite powder particles onto a substrate via a severe plastic deformation mechanism without any significant fusion. To have a successful deposition, the specific powder particles should travel above a material-dependent threshold velocity, which is called the critical velocity. The convergent-divergent nozzle is employed for achieving high velocities. The main objective of the current research is to study the flow visualization of two-phase titanium particle laden nitrogen gas in a simulated 2-D axisymmetric nozzle where particles are having a particle size of 25 microns, and to investigate the suitability of a specific set of cold spraying process parameters for the successful deposition of titanium powder using computational fluid dynamics. For the analysis, a two-equation realizable k-ϵ simulation viscous model was preferred due to its more realistic consideration of the cold spray process and reduced computational cost. Titanium powder particles will be successfully deposited using cold spray when operated at the precise set of process conditions on account of the average particle velocity observed at standoff distance higher than the critical velocity.</p>
30.	<p>From domestic guardian to the national militia: the familial, the national and the middle class in 1980s popular Hindi films D Ray, P Radhakrishnan - National Identities, 2024</p> <p>Abstract: This essay analyzes the theme of domestic anxiety of the Indian middle class in the 1980s through two specific genres of the contemporary popular Hindi films—the family drama and the action adventure. Poised right before the 1990s neoliberal drive in the Indian economy, the 80s middle class—hitherto staid and hermetic – was rattled by an ‘invasive’ global culture, permissiveness, politics of representation, rights and reform. This paper shows that the cinematic resolution of this crisis is a grudgingly lenient orthodoxy negotiating with the limits of cultural inclusion, represented through the questions of agency, gender, class, caste and ethnicity abounding in the middle class domestic sphere. The essay analyzes the middle class problematization of the familial as well as the national in films like Arth (Bhatt, 1982), Agar Tum Na Hote (Tandon, 1983), Souten (Tak, 1983), Shaan (Sippy, 1980) and Mr. India (Kapur, 1987).</p>
31.	<p>From waste to clean energy: an integrated pyrolysis and catalytic steam reforming process for green hydrogen production from agricultural crop residues PP Singh, A Jaswal, A Singh, T Mondal - ACS Sustainable Chemistry & Engineering, 2024</p> <p>Abstract: Biomass holds significant promise as a renewable feedstock for H₂ production. In this study, an integrated biomass pyrolysis and bio-oil catalytic steam reforming approach was explored for hydrogen production from biomass, focusing on a mixture of agricultural crop residues as the feed material. An optimal bio-oil yield of 40.6 wt % was achieved at 450 °C with a heating rate of 10 °C/min during pyrolysis. Using a LaNi_{0.5}Co_{0.5}O₃ catalyst, time-on-stream experiments exhibited a stable bio-oil conversion (80%) and average H₂ yield (60%) over a 12 h period. Furthermore, FESEM and Raman analysis of the spent catalyst revealed considerable coke formation, which contributed to reduced catalytic activity after 5 h. However, coke was predominantly graphitic in nature, which kept the catalyst active over the entire 12 h period despite significant coke coverage.</p>
32.	<p>Impact of large-scale PV-BESS on dynamics of power system oscillatory modes B Sahu, BP Padhy - 3rd International Conference on Energy, Power and Electrical Engineering (EPEE), 2023</p> <p>Abstract: The target of zero carbon emission from electric power generation results in the replacement of fossil-based energy generation by renewable sources. The increase of power electronically interfaced photovoltaic (PV) power plants into power systems causes severe stability problems due to lack of inertia and damping effect. The battery energy storage systems (BESS) at PV stations can be controlled by a virtual inertia controller (VIC) to provide virtual</p>

	<p>inertia and damping support while smoothing the power fluctuations of PV power plant. As BESS with VIC mimics the characteristics of a synchronous generator, the influence of BESS on low-frequency electro-mechanical oscillations (LEO) is significant. This research paper investigates the probabilistic distribution of power systems LEOs for various controller gain of VIC and stochastic variation of solar irradiance under the influence of phase-locked loop (PLL) dynamics. The modal interaction of PLL and virtual inertia controller with power system oscillatory modes are investigated by stochastic eigenvalue analysis using Monte Carlo simulation approach.</p>
33.	<p>Interface-induced origin of Schottky-to-Ohmic-to-Schottky conversion in non-conventional contact to β-Ga₂O₃ D Kaur, R Dahiya, S Shivani, M Kumar - Applied Physics Letters, 2024</p> <p>Abstract: β-Ga₂O₃ is an emerging ultra-wide bandgap semiconductor with wide-ranging applications from civil to military realms. Due to the varied surface states and upward band-bending of β-Ga₂O₃ with most metals, most of the conventional metal contacts turn out to be Schottky in nature, leading to a paucity of suitable Ohmic contacts to Ga₂O₃. Transparent conducting oxides (TCOs) offer the flexibility of conduction along with optical transparency, useful especially for optoelectronic devices. Herein, we report on the use of indium-zinc oxide (IZO), a TCO, as a suitable, unconventional contact to β-Ga₂O₃. The devices show a unique conversion from Schottky to Ohmic by annealing at an optimized temperature of 650 °C, while changing back to Schottky at higher temperatures. At 650 °C, the interface chemistry as studied by x-ray photoelectron spectroscopy changes drastically with band-bending of β-Ga₂O₃ shifting from upward to downward at the interface leading to a type II band alignment, responsible for the Schottky-to-Ohmic conversion. The results provide evidence of using IZO layer as an alternate contact material to β-Ga₂O₃ whose behavior as Ohmic or Schottky contact may be tuned by simply varying the annealing temperature and inducing interfacial changes at the semiconductor-electrode interface, while maintaining excellent device resilience. The proposed conducting oxide layer provides an effective strategy toward control and tunability in nature of contacts toward gallium oxide and its applications for high temperature resilience solar-blind photodetectors.</p>
34.	<p>Intermittent oscillation dynamics in non-premixed swirl flames Y Nanda, S Muralidharan, A Saurabh, L Kabiraj... - AIAA SCITECH 2024 Forum, 2024</p> <p>Abstract: Thermoacoustic instabilities caused by a swirl nozzle which has been optimized for NO_x emissions have been studied in an atmospheric combustor and a staged multi-nozzle lean direct injection combustor which has the operational power of a gas turbine combustor. Type-II intermittency was detected in both systems, the unstable dynamics of the acoustics and the flame arising during the intermittent states have been investigated and compared across the two systems to understand the changes in intermittent behavior with a single nozzle and multiple nozzles. Intermittent combustion oscillations in the atmospheric combustor were also compared with and without an exit plate. Scalar pressure measurements were used for phase space reconstruction of recurrence plots to analyze the non-linear behavior of the instability. Recurrence plots were quantified by the calculation of recurrence rate, determinism, entropy, and averaged line lengths. Spectral proper orthogonal decomposition using time-resolved OH* Chemiluminescence images was performed to extract the complex features of the flame during the instability cycle.</p>
35.	<p>Introduction to bio-nanotechnology R Anand, KK Mishra, N Bharadvaja - Biogenic Nanomaterials for Environmental Sustainability: Principles, Practices, and Opportunities: Book Chapter, 2024</p> <p>Abstract: Nanobiotechnology is the application of nanosized materials in various operational fields of biotechnology. The study of nanotubes, nanoparticles, nanofibers, nanowires, and other such nanometre-ranging structures is called nanoscience. This one billionth fine of a unit possesses properties for applications in various fields like bioremediation, nano-therapy, drug</p>

	<p>delivery, and so on. This book chapter describes the concept, key prospects, and features of bio-nano-technology; the preparation, analysis, characterization, and application of nanomaterials for biological advancements. The major biological fields that benefit from nanotechnology have been briefly discussed.</p>
36.	<p>Investigation of survived solidification features after hot isostatic pressing in third generation γ-TiAl alloys: Ti-45Al-(5, 10)Nb-0.2B-0.2C N Bibhanshu, R Rajanna, A Bhattacharjee... - Metallurgical and Materials Transactions A, 2024</p> <p>Abstract: The effect of niobium (Nb) content in titanium aluminide (TiAl) with the composition Ti-45Al-(5, 10)Nb-0.2B-0.2C manifests in terms of change in the sequence of phase evolution during solidification. In the present investigation, the consequent evolution of microstructure, phases, and crystallographic texture has been examined for the survived solidification features after hot isostatic pressing (HIP). It has been observed that 10 at. pct of Nb in γ-TiAl alloy ensures excellent grain refinement and random texture through the ingot. Because of phase transformation during cooling, the orientation relationship is maintained between the evolved phases. A subdued thermal gradient, related to the basic grain refinement mechanism by constitutional undercooling and by the change of the solidification path, persists during solidification for the two Nb containing alloys and maintains grain growth kinetics at different locations in the ingot. The two different types of γ-γ lamellae have been identified which is related to the two different types of the transformation mechanism. The microhardness also has been investigated from the periphery to the central region of the casted and HIPed circular pancake. A novel mechanism has been proposed for the different types of γ-γ lamellae formation and the mechanism of the crystallographic orientation evolution during the solidification of these alloys.</p>
37.	<p>Investigation on combustion stability, unregulated and particle emissions in RCCI engine RK Yadav, MR Saxena, RK Maurya - SAE Technical Papers, 2024</p> <p>Abstract: This study experimentally investigates the combustion stability in RCCI engines along with the gaseous (regulated and unregulated) and particle emissions. Multifractal analysis is used to characterize the cyclic combustion variations in the combustion parameters (such as IMEP, CA50, Pmax) of the RCCI engine. The investigation is carried out on a modified single-cylinder diesel engine to operate in RCCI combustion mode. The RCCI combustion mode is tested for different fuel premixing ratio (r_p) and diesel injection timing (SOI) at fixed engine speed (1500rpm) and load (1.5 bar BMEP). The particle number characteristics and gaseous emissions are measured using a differential mobility spectrometer (DMS500) and Fourier Transform Infrared Spectroscopy (FTIR) along with Flame Ionizing Detector (FID), respectively. The results indicate that the NO_x emissions decrease with advanced SOI while the methane (CH₄) emission increases. The result shows that advanced SOI and an increase in r_p enhances the formation of unsaturated, saturated and formaldehyde emissions. The nucleation mode particles (NMPs) and total particle number (PN) emission increased with advanced diesel SOI. Multifractal detrended fluctuation analysis (MFDFA) demonstrated a positive correlation between diesel SOI and the level of multifractality. It is found that the time series of combustion parameters exhibits large fluctuations at smaller time scales, while small fluctuations are detected at higher time scales.</p>
38.	<p>KL-DNAS: Knowledge distillation-based latency aware-differentiable architecture search for video motion magnification J Singh, S Murala, GSR Kosuru - IEEE Transactions on Neural Networks and Learning Systems, 2024</p> <p>Abstract: Video motion magnification is the task of making subtle minute motions visible. Many times subtle motion occurs while being invisible to the naked eye, e.g., slight deformations in muscles of an athlete, small vibrations in the objects, microexpression, and chest movement</p>

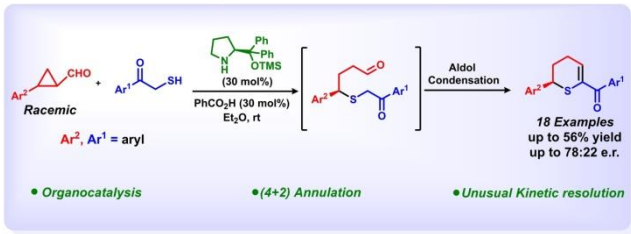
	<p>while breathing. Magnification of such small motions has resulted in various applications like posture deformities detection, microexpression recognition, and studying the structural properties. State-of-the-art (SOTA) methods have fixed computational complexity, which makes them less suitable for applications requiring different time constraints, e.g., real-time respiratory rate measurement and microexpression classification. To solve this problem, we propose a knowledge distillation-based latency aware-differentiable architecture search (KL-DNAS) method for video motion magnification. To reduce memory requirements and to improve denoising characteristics, we use a teacher network to search the network by parts using knowledge distillation (KD). Furthermore, search among different receptive fields and multifeature connections are applied for individual layers. Also, a novel latency loss is proposed to jointly optimize the target latency constraint and output quality. We are able to find smaller model than the SOTA method and better motion magnification with lesser distortions. https://github.com/jasdeep-singh-007/KL-DNAS.</p>
39.	<p>Landfill leachate analysis from selected landfill sites and its impact on groundwater quality, New Delhi, India A Hussain, A Deshwal, M Priyadarshi, S Pathak... - Environment, Development and Sustainability, 2024</p> <p>Abstract: Managing leachates from landfills in India is an important economic and environmental concern. Due to the exponential growth of population, industrialization and urbanization, several types of byproducts have been generated from day-to-day life. These byproducts are dumped in a haphazard or unempirical manner into the open space, which causes an alarming state of problem in developing country like India. In Indian context, in one of the major metro cities like New Delhi, the landfill techniques have been said to be a menace to the health of nearby residents. The present study has been undertaken to assess the environmental hazards that municipal solid waste landfill leachate poses to the groundwater. Three landfill sites, Bhalswa, Okhla, and Ghazipur of New Delhi, have been selected to determine the physicochemical properties, including significant metals of lowland leachate. Furthermore, the leachates from three different dumpyards have been compared with the permissible limits prescribed by Environmental Protection Agency, 1986. Thus, the present research findings focus for the Bhalswa landfill site leachate analysis, which indicates a high biochemical oxygen demand concentration of 3356 mg/L and chemical oxygen demand concentration of 5942 mg/L, respectively. However, the total dissolved solids, electrical conductivity, and ammonical nitrogen concentrations have been 12,384 mg/L, 32,600 $\mu\text{mho/cm}$, and 36.6 mg/L. It is observed that the Ghazipur landfill site was highly tainted as compared to Okhla and Bhalswa landfill sites. Further, quantitative analysis deduces the trend of heavy metals concentration of iron, nickel, zinc, arsenic, and chromium in the order of Bhalswa > Okhla > Ghazipur landfill sites. The toxicity hazard of dumpsites from Bhalswa, Ghazipur, and Okhla was also examined using the leachate pollution index, and the values were obtained such as 21.57, 26.61, and 20.28, respectively. Additionally, the present study reveals that the leachate percolating through all the landfill sites exceeds the permissible limits prescribed by Environmental Protection Agency, 1986, and thus, an immediate attention is required to circumvent its other adverse effect on the nearby area and groundwater reserves.</p>
40.	<p>Low resistance Ohmic contact of multi-metallic Mo/Al/Au stack with ultra-wide bandgap Ga2O3 thin film with post-annealing and its in-depth interface studies for next-generation high-power devices S Dahiya, N Sharma ... M Kumar -Surfaces and Interfaces, 2024</p> <p>Abstract: Ultra-wide band gap materials like β-Ga2O3 is considered as a potential candidate for power devices owing to their high breakdown voltage in contrast to the conventional semiconductors. The performance and the figure-of-merit for power devices critically depend on resistance offered by ohmic contact of metal with ultra-wide gap materials. However, high-quality ohmic contacts with Ga2O3</p>

	<p>presents a significant challenge due to Fermi-level pinning and formation of Schottky barriers for the majority of metal contacts. Here, we investigated the electrical characteristics and interfacial reactions of Au/Al/Mo metal stack with β-Ga₂O₃ thin film at various annealing temperatures to demonstrate the ohmic contact formation mechanism. In-depth surface-sensitive XPS and UPS are employed to study the interface of metallic stack/Ga₂O₃ thin film. Our results indicate that post-annealing at high temperatures led to the intermixing of the metallic stack and results in the formation of binary intermetallic compounds of Al and Au. The intermetallic compound diffuses into the Ga₂O₃ layer and resulting in the creation of an oxygen-deficiency near the interface and helping to achieve contact resistance of $7.15 \times 10^{-6} \Omega\text{-cm}^2$. This study establishes a robust foundation for the expanded utilization of Ga₂O₃ in power electronics and optoelectronics devices, emphasizing the vital role of interface engineering.</p> 
41.	<p>Mapi-Pro: an energy efficient memory mapping technique for intermittent computing SJ Badri, M Saini, N Goel - ACM Transactions on Architecture and Code Optimization, 2023</p> <p>Abstract: Battery-less technology evolved to replace battery usage in space, deep mines, and other environments to reduce cost and pollution. Non-volatile memory (NVM) based processors were explored for saving the system state during a power failure. Such devices have a small SRAM and large non-volatile memory. To make the system energy efficient, we need to use SRAM efficiently. So we must select some portions of the application and map them to either SRAM or FRAM. This paper proposes an ILP-based memory mapping technique for intermittently powered IoT devices. Our proposed technique gives an optimal mapping choice that reduces the system's Energy-Delay Product (EDP). We validated our system using TI-based MSP430FR6989 and MSP430F5529 development boards. Our proposed memory configuration consumes 38.10% less EDP than the baseline configuration and 9.30% less EDP than the existing work under stable power. Our proposed configuration achieves 20.15% less EDP than the baseline configuration and 26.87% less EDP than the existing work under unstable power. This work supports intermittent computing and works efficiently during frequent power failures.</p>
42.	<p>MARS: A multi-view contrastive approach to human activity recognition from accelerometer sensor G Sharma, A Dhall, R Subramanian - IEEE Sensors Letters, 2024</p> <p>Abstract: In this letter, we present MARS , a novel approach which combines a multi-view fusion technique with contrastive loss to accurately identify human activities using accelerometer sensor data. Accelerometer sensor enables precise monitoring of human activities in diverse contexts. Our approach leverages both temporal and spectral views of accelerometer data, integrating them through an attention mechanism to enhance the overall understanding of human activities. To further improve the discriminative power of the learned representations corresponding to different activity classes, we apply a contrastive loss-based siamese network. Empirical findings confirm that MARS outperforms state-of-the-art on the harAGE dataset by a significant margin of 4.71 in unweighted average recall.</p>
43.	<p>Metallic functionally graded materials K Kumar, K Rakha, S Reza, H Singh – Modern Materials and Manufacturing Techniques: Book Chapter, 2024</p> <p>Abstract: A paradigm shift is underway where pure classical materials, alloys, and conventional composites are being replaced by functionally graded materials (FGMs) for numerous applications in biomedical, aerospace, turbomachinery, and structural engineering. FGMs are beneficial for the components being operated in varying service conditions across their geometry, as different material</p>


	<p>properties are required at different locations on them. These materials are designed with spatial variation in properties (chemical, mechanical, magnetic, thermal, and electrical) by systematically coordinating with the functional requirement. The properties are tailored by varying one or more of the microstructure, porosity, and chemical composition at a time. The evolution of functionally graded additive manufacturing (FGAM) has transformed the modelling from geometric characteristics to performance basis by imparting performance-steered functionality to objects. Furthermore, integrating the opportunistic and restrictive aspects of additive manufacturing can enhance the design attributes like novelty and quality. The present study put forth a theoretical understanding of FGMs by summarizing the current modelling and optimization methods, fabrication, post-processing techniques, and characterization tools. In addition, the potential strategies to overcome various technological barriers and future research opportunities are demonstrated. Being a state-of-the-art and comprehensive review, it can be helpful for both academia and industry.</p>
44.	<p>Model-based safe reinforcement learning using variable horizon rollouts S Gupta, U Suryaman, R Narava, SS Jha - Proceedings of the 7th Joint International Conference on Data Science & Management of Data (11th ACM IKDD CODS and 29th COMAD), 2024</p> <p>Abstract: Safe reinforcement learning aims to ensure the safety of agents and their interactions with the environment. Traditional reinforcement learning algorithms often neglect safety considerations, resulting in undesirable consequences when deployed in real-world scenarios. To address this issue, safe reinforcement learning algorithms incorporate safety constraints or modify the reward distribution to prioritize the safety of the agent. Recent literature on model-based safe reinforcement learning uses a fixed look-ahead horizon to avoid unsafe states, limiting the agent's adaptability to changing environments. In this paper, we propose a variable horizon look-ahead based on the agent's current state, resulting in improved performance and adaptability in uncertain environments. Our approach leverages the Gaussian process regression model to estimate the value of the horizon dynamically based on the agent's current state. To enhance sample efficiency, we introduce a selective sampling strategy that reduces the number of rollouts by eliminating samples that may lead to unsafe states and also optimizes the use of computational resources while ensuring safety. We evaluate the effectiveness of our approach in multiple mujoco environments. Our results demonstrate a significant reduction in terms of safety violations during validating compared to existing approaches from the literature.</p>
45.	<p>Modeling root zone water and salt transport using matric flux potential based root water uptake distribution A Kumar, I Sonkar, R Sarmah - Journal of Hydrology, 2024</p> <p>Abstract: It is important to delineate the root water uptake (RWU) response to salt and water stress for assessing future water availability under extreme climatic conditions. The process of RWU in salt-affected soils is highly complex and not well understood. The present study proposed a matric flux potential based non-linear RWU model capable of calculating reduced RWU in water and salt stressed conditions. The study incorporates a sensitivity analysis of the model's parameters. For the inverse estimation of these parameters, an objective function has been formulated, utilizing data derived from the highly sensitive model's response. The proposed objective function provides unique estimates for these parameters. Using this objective function in an optimization process, the model is calibrated with observed data obtained from a soil column lysimeter experiment conducted on berseem crop (<i>Trifolium alexandrinum</i>). The parameters are optimized through the coupling of the model with a genetic algorithm-based optimizer tool. Simulated data for soil moisture, electrical conductivity, and percolation are then compared to observed data. The simulated model's responses are found to be closely aligns with the experimentally observed values. The RWU under four irrigation of different salinity levels is simulated. The results highlight a reduction in RWU compensation under high-salinity irrigation treatment.</p>
46.	<p>Momentum transport of morphological instability in fluid displacement with changes in viscosity</p>

	<p>T Ban, H Ishii... M Mishra... - Royal Society of Chemistry, 2024</p> <p>Abstract: Saffman–Taylor instability exhibits a stepwise unstable morphology from a stable interface to viscous fingering, eventually leading to tip splitting. The nonlinear dynamics of the destabilized interface depends on various flow properties. However, the physicochemical mechanism that determines the transition point of the flow state is unclear. We studied the interfacial instability transition in miscible displacement from a thermodynamic perspective by calculating the momentum transport and entropy production. Using numerical analysis based on Darcy's law coupled with the convection-diffusion equation, the observed flux-dependent flow state transitions were attributed to the selection of the flow state with a higher entropy production.</p>
47.	<p>NEAT activity detection using smartwatch A Dewan, V.M.V. Gunturi, V Naik - International Journal of Ad Hoc and Ubiquitous Computing, 2024</p> <p>Abstract: This paper presents a system for distinguishing non-exercise activity thermogenesis (NEAT) and non-NEAT activities at home. NEAT includes energy expended on activities apart from sleep, eating, or traditional exercise. Our study focuses on specific NEAT activities like cooking, sweeping, mopping, walking, climbing, and descending, as well as non-NEAT activities such as eating, driving, working on a laptop, texting, cycling, and watching TV/idle time. We analyse parameters like classification features, upload rate, data sampling frequency, and window length, and their impact on battery depletion rate and classification accuracy. Previous research has not adequately addressed NEAT activities like cooking, sweeping, and mopping. Our study uses lower frequency data sampling (10 Hz and 1 Hz). Findings suggest using statistical features, sampling at 1 Hz, and maximising upload rate and window length for optimal battery efficiency (33,000 milliamperes per hour, 87% accuracy). For highest accuracy, use ECDF features, sample at 10 Hz, and a window length of six seconds or more (37,000 milliamperes per hour, 97% accuracy).</p>
48.	<p>Next-generation therapies for type 2 diabetes mellitus D Patra, S Roy, P Ramprasad, D Pal - Functional Smart Nanomaterials and Their Theranostics Approaches: Book Chapter, 2024</p> <p>Abstract: Type 2 diabetes mellitus (T2DM), which has been considered a pandemic due to its growing pervasiveness in the world population, is associated with obesity, ageing, a sedentary lifestyle, and the complex interplay of genetic and environmental factors. Globally, adult diabetic cases hit 537 million in 2021 and escalated to approximately a billion by 2045. In T2DM, the metabolic pathophysiological state impairs insulin sensitivity, glucose tolerance, β-cell functionality, and immune-metabolic harmony and introduces dysfunction of insulin-responsive tissues. Research in the biomedical discipline innovates a plethora of anti-diabetic therapeutic candidates, but very few are clinically successful, although drug delivery, immunological approaches, oligonucleotide therapy, and regenerative and transplantation medicines contribute to a wide range of therapeutic dimensions. Therefore, understanding this complex pathophysiological state needs to be extensively studied, and new molecules are required to be revealed at the earliest. In this chapter, we have precisely discussed the recently developed and potent, underdeveloped therapies for the treatment of T2DM. Participation of analogues, agonists, antagonists, activators, and inhibitors targeting specific components in the context of insulin resistance (IR) holds promise for addressing both IR and T2DM. Additionally, we delve into the exploration of newly developed immune-based therapies and diverse approaches for administering insulin to individuals with T2DM.</p>
49.	<p>Numerical investigation on hydrogen enrichment and EGR on in-cylinder soot and nox formation in dual-fuel CI-Engine NK Yadav, RK Maurya - SAE Technical Papers, 2024</p>

	<p>Abstract: To mitigate the NO_x emissions from diesel engines, the adoption of exhaust gas recirculation (EGR) has gained widespread acceptance as a technology. Nonetheless, employing EGR has the drawback of elevating soot emissions. The use of hydrogen-enriched air with EGR in a diesel engine (dual-fuel operation), offers the potential to decrease in-cylinder soot formation while simultaneously reducing NO_x emissions. The present study numerically investigates the effect of hydrogen energy share and engine load on the formation and emission of soot and NO_x emission from hydrogen-diesel dual-fuel engine. The numerical investigation is performed using an n-heptane/H₂ reduced reaction mechanism with a two-step soot model in ANSYS FORTE. To enhance the accuracy of predicting dual-fuel combustion in a hydrogen-diesel dual-fuel engine, a reduced n-heptane reaction mechanism is integrated with a hydrogen reaction mechanism using CHEMKIN. The study concludes that hydrogen enrichment plays a significant role by decreasing the soot precursor concentration by increasing the hydroxyl (OH) radical and suppressing soot formation by enhancing oxidation. Hydrogen enrichment in dual-fuel operation results in a significant reduction in soot and NO_x emissions significantly under low load conditions. The addition of hydrogen in diesel engine results in decreases in the concentration of acetylene (C₂H₂), propyne (C₃H₄) locally inside the combustion chamber which inhibits the formation of soot.</p>
50.	<p>Numerical simulation of bending and length-varying flapping wing using discrete vortex method R Kumar, D Samanta - International Journal of Modern Physics C, 2023</p> <p>Abstract: The paper aims to perform numerical simulations of flapping flight using Discrete Vortex Method (DVM) scheme. The scheme is suitable for moderately low Reynolds number (≤ 105) and computationally less expensive as the flow domain doesn't need to be discretized at each time step. Flapping of a one-dimensional (1D) flexible filament in a two-dimensional (2D) inviscid flow is simulated. The effect of bending by varying the wing shape along the spanwise length on aerodynamic performance was studied. It is observed that compared to rigid wings, bending wings are found to be better in generating lift. The effect of various bending wing configurations (F1, F2, F3 and F4) and different methods of imposing the bending (W1, W2 and W3) is studied. It was demonstrated that applying wing bending only during the downstroke phase (W2) is more effective than imposing bending throughout the flapping cycle (W1). Moreover, an effort is made to replicate the bending configuration observed in manta ray fish (W3) to investigate its impact on flow domain characteristics, lift, and thrust forces. Furthermore, the inclusion of a winglet is found to significantly enhance lift generation. In addition to the study of bending effects on aerodynamic performance, the study also seeks to emulate a unique aspect of bat flight kinematics, specifically the dynamic variation in wing span length during flapping. In a comparative analysis of two span length variation strategies, it is discerned that exclusively varying span length during the upstroke phase is the optimal approach for achieving increased lift generation. The study highlights the crucial role of wing bending and span length modulation in achieving elevated lift forces while simultaneously reducing drag. These findings are seen as holding significant promise for the design and optimization of Micro Air Vehicles (MAVs) utilizing flapping-based lift generation mechanisms, contributing substantially to the identification of optimal parameters for enhancing MAVs' aerodynamic performance and operational efficiency.</p>
51.	<p>Online algorithm for clustering with capacity constraints S Gupta, S Jain, NC Krishnan... - CODS-COMAD '24: Proceedings of the 7th Joint International Conference on Data Science & Management of Data (11th ACM IKDD CODS and 29th COMAD), 2024</p> <p>Abstract: Traditional clustering often results in imbalanced clusters, limiting its suitability for real-world problems. In response, capacitated clustering methods have emerged, aiming to achieve balanced clusters by limiting points in each cluster. In this paper, we introduce online</p>

	algorithms with provable bounds on opened centers and cost approximation. We validate our methods experimentally.
52.	<p>Organocatalytic enantioselective (4+2) annulation of cyclopropane carbaldehydes with 2-mercapto-1-arylethanones N Yadav, A Hazra, P Singh, P Banerjee - Advanced Synthesis & Catalysis, 2024</p> <p>Abstract: Here, we report the organocatalytic enantioselective synthesis of dihydrothiopyran derivatives from trans racemic donor-acceptor cyclopropane carbaldehydes (DACCs) and 2-mercapto-1-arylethanone via formal thio (4+2) cycloaddition involving thia-Michael aldol condensation and annulation. Mechanistic studies indicate a typical kinetic resolution (KR) is involved in this transformation, which results in moderate yields and enantiomeric ratios. Remarkably, this method is characterized by its one-pot simplicity, mild reaction conditions, and resilience towards air and moisture interference.</p>  <p>• Organocatalysis • (4+2) Annulation • Unusual Kinetic resolution</p> <p>18 Examples up to 56% yield up to 78:22 e.r.</p>
53.	<p>Out-of-equilibrium dynamics of Bose-Bose mixtures in optical lattices P Kaur, K Suthar, D Angom, S Gautam - Physical Review A, 2024</p> <p>Abstract: We examine the quench dynamics across quantum phase transitions from a Mott insulator (MI) to a superfluid (SF) phase in a two-component bosonic mixture in an optical lattice. We show that two-component Bose mixtures exhibit qualitatively different quantum dynamics than one-component Bose gas. In addition to second-order MI-SF transitions, we investigate quench dynamics across a first-order MI-SF phase boundary. The Bose mixtures show the critical slowing down of dynamics near the critical transition point, as proposed by the Kibble-Zurek mechanism. For MI-SF transitions with homogeneous lattice-site distributions in the MI phase, the dynamical critical exponents extracted by the power-law scaling of the proposed quantities obtained via numerical simulations are in very close agreement with the mean-field predictions.</p>
54.	<p>Probing topological charge of discrete vortices V Dev, V Pal - Physical Review Applied, 2023</p> <p>Abstract: A discrete vortex, formed by a one-dimensional (1D) ring array of lasers, has high output power as compared with a conventional continuous vortex, and therefore has attracted considerable interest due to widespread applications in various fields. We present a method for probing the magnitude and sign of the topological charge (l) of an unknown discrete vortex, by analyzing the interference pattern of a 1D ring array of lasers. The interference pattern of an unknown discrete vortex with $l \neq 0$ is averaged with the interference pattern corresponding to $l=0$, which gives rise to a variation in the fringe visibility as a function of the laser number (j) in a 1D ring array. The number of dips observed in the fringe-visibility curve is found to be proportional to the magnitude of the topological charge of a discrete vortex. After determination of the magnitude, the sign of $l \neq 0$ is determined by averaging its interference pattern with the interference pattern corresponding to $l=1$. The number of dips in the fringe-visibility curve decreases by 1 for positive l values and increases by 1 for negative l values. Further, we verify our method against the phase disorder, and it is found that the phase disorder does not influence accurate determination of the topological charge of a discrete vortex. The working principle as well as numerical and experimental results are presented for discrete vortices with topological charges from small to large values. Excellent agreement between the experimental results and the numerical simulations is found. Our method can be useful in applications of discrete vortices especially where conventional continuous vortices have power limitations.</p>

55.	<p>Propagation of nonlinear surface waves over non-periodic oscillatory bottom profiles D Goyal, TK Hota, SC Martha - European Journal of Mechanics-B/Fluids, 2024</p> <p>Abstract: The effect of non-uniform, oscillating bottom profiles on a two-layer stable density stratification model has been examined using the method of weakly non-linear analysis. The study of bottom profiles in the context of two-layered stratified fluids has focused on three specific types: (a) profiles that exhibit a monotonically decreasing pattern, (b) profiles that decay exponentially, and (c) profiles that display Gaussian oscillations. The analysis of the second-order reflection and transmission coefficients for the nonlinear boundary value problem was conducted using a combination of the regular perturbation method and the Fourier transforms technique. The numerical findings pertaining to various physical parameters have been presented, demonstrating the impact of the Class I Bragg resonance in all three profiles and the elevation of the tails in the monotonically decreasing oscillatory profile. Specifically, the presence of high reflections due to the tail-lifting phenomenon is observed in a profile that exhibits a monotonically decreasing pattern, in contrast to the other profiles. The findings of the study indicate that interface modes demonstrate pronounced reflections when the density ratios are low, but divergent results are observed when the density ratios are high. As the density ratio R increases, there is a greater migration of wave energy from the interface mode to the surface mode, resulting in increased levels of reflection. As the value of R approaches 1, it is observed that lower frequencies exhibit significantly more pronounced internal mode reflections compared to surface mode. Several contrasting aspects can be observed in three oscillatory profiles when compared to periodic profiles. These aspects include the disappearance of zero reflection, also known as complete transmission, as well as the absence of oscillations. The findings of this study demonstrate that a monotonically oscillating decreasing profile can be considered as an efficacious Bragg breakwater. Furthermore, this study investigates the energy transfer that occurs during the movement of surface and internal waves across non-periodic oscillatory profiles. As a result, an energy balance relationship is derived, which specifically applies to surface and interface modes. This work has hydrodynamical relevance to wave propagation in coastal regions and to the hydrodynamics of tsunamis in the open ocean, both of which are affected by changes in the bathymetry of the fluid region.</p>
56.	<p>Pyrene-based nanoporous covalent organic framework for carboxylation of C–H bonds with CO₂ and value-added 2-oxazolidinones synthesis under ambient conditions G Singh, N Duhan, TJ D Kumar, CM Nagaraja - ACS Applied Materials & Interfaces, 2024</p> <p>Abstract: The selective carbon capture and utilization (CCU) as a one-carbon (C1) feedstock offers dual advantages for mitigating the rising atmospheric CO₂ content and producing fine chemicals/fuels. In this context, herein, we report the application of a porous bipyridine-functionalized, pyrene-based covalent organic framework (Pybpy-COF) for the stable anchoring of catalytic Ag(0) nanoparticles (NPs) and its catalytic investigation for fixation of CO₂ to commodity chemicals at ambient conditions. Notably, Ag@Pybpy-COF showed excellent catalytic activity for the carboxylation of various terminal alkynes to corresponding alkynyl carboxylic acids/phenylpropionic acids via C–H bond activation under atmospheric pressure conditions. Besides, carboxylative cyclization of various propargylic amines with CO₂ to generate 2-oxazolidinones, an important class of antibiotics, has also been achieved under mild conditions. This significant catalytic activity of Ag@Pybpy-COF with wide functional group tolerance is rendered by the presence of highly exposed, alkynophilic Ag(0) catalytic sites decorated on the pore walls of high surface area (787 m² g^{−1}) Pybpy-COF. Further, density functional theory calculations unveiled the detailed mechanistic path of the Ag@Pybpy-COF-catalyzed transformation of CO₂ to alkynyl carboxylic acids and 2-oxazolidinones. Moreover, the catalyst showed high recyclability for several cycles of reuse without significant loss in its catalytic activity and structural rigidity. This work demonstrates the promising application of Pybpy-COF for stable anchoring of Ag NPs for successful transformation of CO₂ to valuable</p>

	<p>commodity chemicals at ambient conditions.</p> 
57.	<p>Quantitative analysis of hydropower potential in the upper Beas basin using geographical information system and MIKE 11 nedbor afrstromnings model (NAM) M Kumar, RK Tiwari, K Kumar, KS Rautela, S Safi – Ecohydrology, 2024</p> <p>Abstract: The present study aims to identify potential locations for small-scale hydroelectric power (HEP) stations in hilly regions for the purpose of generating renewable energy. A rainfall-runoff (R-R) model of the Beas River catchment was established using the MIKE 11 NAM to estimate the available discharge. The model was calibrated and validated over the period of June-2015–May-2018 and June-2018–May-2020, respectively, using daily observed discharge data at the Pandoh Dam site. The model exhibited good performance with a coefficient of determination (R²) of 0.82 during calibration and 0.70 during validation and a water balance of –0.01% and –18%, respectively. However, Lmax, CK1, CK2 and CQOF are found most sensitive parameters during the calibration. Further, thirteen major streams of order five or higher were selected for the assessment of hydropower potential, resulting in the identification of 131 potential run-of-river (ROR) hydropower sites. The hydropower potential at two proposed sites, Bhang SHEP (9 MW) and Raison SHEP (18 MW), was estimated to be 11 and 15 MW, respectively, using 90% dependable flow. The results demonstrate the effectiveness of using Digital Elevation Model (DEM) and Geographic Information System (GIS) techniques for determining hydropower potential in ungauged basins in the Himalayas.</p>
58.	<p>Radiation effect on stagnation point flow of Casson nanofluid past a stretching plate/cylinder US Mahabaleshwar, T Maranna, M Mishra, M Hatami, B Sunden - Scientific Reports, 2024</p> <p>Abstract: The exclusive behaviour of nanofluid has been actively emphasized due to the determination of improved thermal efficiency. Hence, the aim of this study is to highlight the laminar boundary layer axisymmetric stagnation point flow of Casson nanofluid past a stretching plate/cylinder under the influence of thermal radiation and suction/injection. Nanofluid comprises water and Fe₃ O₄ as nanoparticles. In this article, a novel casson nanofluid model has been developed and studied on stretchable flat plate or circular cylinder. Adequate rational assumptions (velocity components) are employed for the transformation of the governing partial-differential equations into a group of non-dimensional ordinary-differential formulas, which are then solved analytically. The momentum and energy equations are solved through the complementary error function method and scaling quantities. Using various figures, the effects of essential factors on the nanofluid flow, heat transportation, and Nusselt number, are determined and explored. From obtained results, it is observed that the velocity field diminishes owing to magnification in stretching parameter B and Casson fluid parameter Λ. The temperature field increases by amplifying radiation N_r, and solid volume fraction parameter ϕ. The research is applicable to developing procedures for electric-conductive nanomaterials, which have potential applications in aircraft, smart coating transport phenomena, industry, engineering, and other sectors.</p>
59.	<p>Real-time screening of Ni x B y bifunctional electrocatalysts for overall NH 3 synthesis via SG-TC SECM D Gupta, A Kafle, M Singh, S Kumar, TC Nagaiah - Materials Horizons, 2024</p> <p>Abstract: Electrochemical ammonia synthesis, which couples oxygen evolution at the anode with nitrogen reduction at the cathode, holds great significance for future food and energy needs.</p>

	<p>Both of these half-cell reactions determine the overall cell potential and efficiency of the process. However, the employment of different catalysts on either side, due to discrete mechanisms, increases the complexity and material processing costs of the system, where the designing of a bifunctional catalyst active towards both the NRR and OER is of huge significance. Unfortunately, the initial screening of the designed catalysts via physical characterizations, optical methods and other techniques, does not provide details about the electrochemical activity. The scanning electrochemical microscopy (SECM) technique can be useful to screen multi-catalysts at the same time for their electrochemical activities. Herein, we employed the sample generation-tip collection (SG-TC) mode of SECM to screen the designed Ni_xB_y catalysts before half-cell investigations, which suggested that the catalyst synthesized via sonochemical reduction (SR), i.e. Ni_xB_y (SR), was a better catalyst. This inference was in accordance with the half-cell NRR and OER measurements (FE: 49% for NH_3 production, OER overpotential: 300 mV). By virtue of this remarkable bifunctional activity, the NRR-OER coupled full cell was assembled, which initiated the NH_3 production at just 1.7 V and produced NH_3 ($1.08 \text{ mg h}^{-1} \text{ mg}_{\text{cat}}^{-1}$) at the cathode and O_2 ($0.81 \text{ mg h}^{-1} \text{ mg}_{\text{cat}}^{-1}$) at the anode after 2 h of electrolysis at 1.9 V.</p>
60.	<p>SCE: Shared concept extractor to explain a CNN's classification dynamics V Kamakshi, NC Krishnan - CODS-COMAD '24: Proceedings of the 7th Joint International Conference on Data Science & Management of Data (11th ACM IKDD CODS and 29th COMAD), 2024</p> <p>Abstract: To better understand how accurate opaque black box models work, it is necessary to explain their internal workings in terms of human-interpretable image sub-regions known as concepts. This explanation will provide insights into how these models perceive the sharedness of concepts across related classes, as frequently observed in the real world. With this objective in mind, the proposed work aims to leverage an incremental Non-negative Matrix Factorization technique to extract shared concepts in a memory-efficient manner, thereby reflecting the sharedness of concepts across classes. The relevance of the extracted concepts towards prediction, as well as the encoding of primitive image aspects such as color, texture, and shape by the concept, will be estimated after training the concept extractor. This approach reduces training overhead and simplifies the explanation pipeline, enabling the elucidation of various concepts - some genuine, some spurious - on which different black box architectures trained on the Imagenet dataset group and distinguish related classes.</p>
61.	<p>Secrecy capacity of hybrid FSO-RF communication links HK Sharma, B Kumbhani - Journal of Optics, 2024</p> <p>Abstract: In this paper, we analyze the secrecy capacity of hybrid communication links comprising cascaded free space optical (FSO) and radio frequency (RF) wireless systems. We consider the system in which FSO links are used as the medium of data transmission for the first hop followed by RF links for relaying the data to the destination. We consider Gamma-Gamma distributed channel gain for the FSO links and Nakagami-m fading distribution for the RF communication link. This takes care of both the line of sight (LOS) and non-LOS conditions for the RF link. We derive closed-form expressions for end-to-end secrecy capacity. The closed-form expressions are derived by representing the incomplete gamma function in the form of Meijer's G-function. Further, closed-form solutions to the integrals involving the product of two Meijer's G-functions are obtained. The analytical expressions have been validated through results obtained from simulations. A close agreement between the simulation and the analytical results is observed.</p>
62.	<p>Simulation of exceptional-point systems on quantum computers for quantum sensing C Waghela, S Dasgupta - AVS Quantum Science, 2024</p> <p>Abstract: There has been debate around applicability of exceptional points (EPs) for quantum sensing. To resolve this, we first explore how to experimentally implement the non-Hermitian</p>

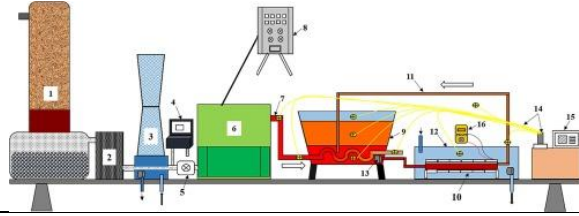
	<p>non-diagonalizable Hamiltonians, which exhibit EPs, in quantum computers that run on unitary gates. We propose to use an ancilla-based method in this regard. Next, we show how such Hamiltonians can be used for parameter estimation using quantum computers and analyze its performance in terms of the quantum Fisher information (QFI) at EPs, both without noise and in the presence of noise. It is well known that QFI of a parameter to be estimated is inversely related to the variance of the parameter by the quantum Cramer-Rao bound. Therefore, the divergence of the QFI at EPs promises sensing advantages. We experimentally demonstrate in a cloud quantum architecture and theoretically show, using Puiseux series, that the QFI indeed diverges in such EP systems that were earlier considered to be non-divergent.</p>
63.	<p>Spatially arranged relay coils to improve the misalignment tolerance at an enhanced transfer distance S Jain, A Bharadwaj, A Sharma - IEEE Transactions on Antennas and Propagation, 2024</p> <p>Abstract: Wireless power transfer systems use relay coils to increase output power over longer distances. This paper presents a novel arrangement of distributed relay coils that improves lateral misalignment tolerance at high transfer distances. The relay coils are optimized using techniques based on a magnetic field forming method by employing an EM simulator to determine the position and geometrical parameters of the relay coils. The optimized design consists of five relay coils, four above the transmitter coil's periphery and one above the center. The proposed design enhances the uniformity of the magnetic field in the receiver region, enabling greater freedom in receiver coil displacement. The authors evaluated the design's performance based on the achieved uniformity factor of the magnetic field and mutual inductance, which are determined as $UF_H = 61.22\%$ and $UF_M = 15.28\%$, respectively, at a transfer distance of 100 mm. The authors fabricated the relay coils using Litz wire on a transparent arsenic sheet at different heights to validate the proposed design. After that, the magnetic field, transmission coefficient (S_{21}), and power transfer efficiency profiles are experimentally measured. The measured results are found to be consistent with the simulated findings, demonstrating the effectiveness of the proposed relay coil arrangements.</p>
64.	<p>Synthesis and characterization of low-friction W-V-N alloy coatings using reactive magnetron sputtering technique for tribological applications AU Rao, SK Tiwari, N Sardana... - Journal of Vacuum Science & Technology A, 2024</p> <p>Abstract: In recent years, self-lubricating hard coatings have garnered significant interest across various industries such as cutting tools, molds, and manufacturing because of their ability to reduce friction and wear at high temperatures in dry-cutting applications. The present study focuses on synthesis of tungsten-vanadium-nitride (W-V-N) coatings using the reactive magnetron cosputtering technique in an $Ar+N_2$ plasma gas environment. The coating microstructure, surface morphology, wetting behavior, and mechanical properties were characterized by grazing incidence x-ray diffraction, field-emission scanning electron microscopy, atomic force microscopy, energy-dispersive spectroscopy, and nanoindentation. Wear resistance properties of the prepared W-V-N alloy coatings were investigated using a ball-on-disk tribometer at two different temperatures. The findings indicate that all W-V-N coatings, regardless of the vanadium content, exhibit a face-centered cubic structure and form a solid solution of W-V-N. Among the coatings studied, W0.68V0.32N exhibited the highest hardness (14.25 GPa) and Young's modulus (257.53 GPa), as well as an excellent wear resistance. Increasing the vanadium content in the W-V-N coating led to a notable reduction in both the specific wear rate and friction coefficient. Moreover, this reduction was more pronounced with an increase in temperature during the wear test. Improvement in the wear properties can be attributed to the formation of Magnéli phases of vanadium oxides on the surface of the coatings. The ability of the W-V-N coating to reduce friction and wear, combined with its improved mechanical properties, makes it a promising candidate for solid lubricating coatings in</p>

	tribological applications.
65.	<p>Synthesis of γ-Valerolactone from Levulinic Acid with Co/NC, and from Furfural via Cascade Reaction Using Co/NC and H-Beta A Chauhan, R Bal, R Srivastava - Energy & Fuels, 2024</p> <p>Abstract: γ-Valerolactone (GVL) has transpired as an ecofriendly solvent, a promising fuel additive, and a precursor to valuable chemicals. The study explores an approach to GVL synthesis by employing non-noble metals in contrast to conventional methods involving noble metals. The selective hydrogenation of levulinic acid (LA) and levulinate esters offers a pathway to GVL production, while the direct transformation from furfural (FA) enhances its potential. The study focuses on 3d transition metal-based N-doped carbon catalysts, highlighting Co/NC as the most effective catalyst for LA to GVL hydrogenation, yielding ~100% GVL. The catalyst was also employed in a one-pot, three-step cascade reaction: FA hydrogenation to furfuryl alcohol (FOL) was performed using 10% Co/NC, ethanolysis of FOL to ethyl levulinate (EL) was facilitated by H-β, and EL hydrogenation to GVL was performed using 10% Co/NC. Each step was optimized independently. The cascade reaction was executed at 140 °C for 12 h through a comprehensive approach, achieving a noteworthy 92.1% GVL yield from FA, which was further upcycled to the gram scale, offering 86% of the final GVL yield. The catalyst characterization, catalytic activity data, and control experiments culminate in the proposed LA to GVL transformation mechanisms and the one-pot, three-step cascade FA to GVL conversion. The research significantly contributes to advancing sustainable GVL production and its multifaceted applications.</p>
66.	<p>The effect of a parabolic apodizer on improving the imaging of optical systems with coma and astigmatism aberrations ANK Reddy, V Dev, V Pal... - Photonics, 2023</p> <p>Abstract: We present the results of improving resolution in the imaging of two closely spaced point sources with an optical system under the influence of apodization and different types of aberrations. In particular, we consider the effect of coma and astigmatism, which are well-known aberrations that can deteriorate the resolution of an optical imaging system. Furthermore, a parabolic apodizer was included in an optical system to improve its imaging capabilities. We found that the two-point imaging performance of an optical system with a parabolic apodizer strongly depends on the coherence conditions of incident light. Furthermore, to analyze the efficiency of the parabolic apodizer, we compared the results of two-point imaging obtained with apodized and unapodized optical systems for distances between the two-point sources, less than or equal to the diffraction limit of an optical system. Moreover, the results of imaging the USAF chart with a parabolic apodizer are presented to show the apodizer's efficacy in single-object imaging. Our results can be applied to the imaging of closely moving structures in microscopy, resolving dense spectral lines in spectroscopy experiments, and developing systems useful for resolving the images of closely associated far-distance objects in astronomical observations.</p>
67.	<p>The saving-investment relationship revisited: new evidence from regime-switching cointegration approach SR Behera, L Mallick, T Mishra - International Economic Journal, 2024</p> <p>Abstract: This paper exploits the regime-switching threshold cointegration approach to elicit the dynamics in the saving-investment relationship and capital mobility in India. Empirical results offer key insights into the threshold cointegration between the saving and investment rates. We find that the adjustment in investment rate in the upper regime is faster than in the lower regime, indicating the higher mobility of capital in the upper regime. Further, results reveal the absence of firm evidence of long-run vs. short-run asymmetries between saving and investment rates. However, results suggest that cumulative positive and negative sums of saving rates affect</p>

	<p>investment rates. We have made adjustments to cyclical and trend patterns in our data using Hamilton's (2018) filter and have produced robust results with regard to asymmetric cointegration. The posterior estimation results suggest that a downward trend in the saving rates substantially impacts the investment rates, and widening the gap between saving and investment rates facilitates huge mobility of international capital in the long run.</p>
68.	<p>Towards digital twin of crops for growth modelling using virtual reality K Singh, M Saini - Proceedings of the 5th ACM International Conference on Multimedia in Asia, 2023</p> <p>Abstract: A major problem that a farmer faces, while adopting a new crop variety in the farm; is the uncertainty associated with its growth. Farmers working on real farms are not aware of the growth models, even for the existing crops. Hence, there is a need for more accessible and intuitive models. This work is a step towards the realization of another promising model, which is the digital twin of a crop. A primary requirement of the digital twin is the digital representation of the crop itself. Extending that notion, the work discusses the development of 3D assets of crops and their temporal alignment. It also describes the methodology involved in the development of a VR framework, which stores the ideal growth of a crop. This framework could be useful to farmers who want to confirm the growth of their crops. Furthermore, it also proposes a quantitative metric to evaluate the VR framework. The consistency of this proposed metric is further backed by a user study which is based on a qualitative method.</p>
69.	<p>Tumor microenvironment regulates immune checkpoints: emerging need of combinatorial therapies M Kalia, K Bhavya, D Pal - Current Tissue Microenvironment Reports, 2024</p> <p>Abstract: Purpose of Review: The tumor microenvironment (TME) acts as a protagonist in the regulation of immune-mediated checkpoints, which contributes to cancer cell immune evasion. This study investigates the dynamic interactions within the TME, with an emphasis on immune checkpoint modulation as a critical mechanism for tumor immune evasion. We investigate the rationale for concurrently targeting numerous checkpoints in order to restore and strengthen anticancer immunity. By comprehensively assessing the current state of research, we highlight the emerging need for integrated immunotherapeutic strategies that address the complex TME-mediated regulation of immune checkpoints, ultimately offering more effective and durable treatment options for cancer patients. Recent Findings: Novel checkpoints such as the B7-H3, B7-H4, and drugs targeting CD73 and SIRPα are being extensively explored. Targeting these checkpoints has reduced the tumor burden by targeting the tumor microenvironment. Summary: We have briefly outlined the tumor microenvironment and the complex signaling cascade it undertakes to fuel cancer growth thereby prompting the need to target the tumor microenvironment through novel checkpoints thus providing tailor-made therapeutic strategies.</p>
70.	<p>Uncertainty principle for Weyl transform and Fourier–Wigner transform A Samanta, S Sarkar - Colloquium Mathematicum, 2023</p> <p>Abstract: We prove an uncertainty type principle for finite linear combinations of Fourier–Wigner transforms. This is equivalent to proving a finite rank theorem for the Weyl transform.</p>
71.	<p>Understand and quantify the consumers' cognitive behavior for the appropriateness features of product aesthetics through the eye-tracking technique J Singh, P Sarkar - International Journal on Interactive Design and Manufacturing (IJIDeM), 2023</p> <p>Abstract: Product design goes beyond mere enclosure; it communicates a product's functionality and utilitarian features. A product's appeal, appropriateness, and beauty act as pivotal links between consumers and their choices. This study delves into the quantification of the appropriateness feature in product aesthetics and its profound influence on human visual and</p>

	<p>cognitive processes. Examining a diverse array of beverage bottle silhouettes, our two-phase study, involving six experts and over 300 participants, brings forth compelling revelations. In phase I, the Frequency Match Ratio (FMR) analysis underscores consumers' adept understanding of function perception during the visual matching of specific silhouettes. Notable examples include the remarkable match ratios achieved for alcohol bottle silhouette P2 (94.71%) and carbonated drink bottle silhouette P5 (85.88%). Furthermore, phase-II, the eye-tracking results revealed several significant findings. Gender-related differences in pupil diameter were noted, with males showing distinct variations, potentially influenced by the robust shapes of alcohol bottles, and females displaying fluctuations, suggesting familiarity with certain bottle designs, particularly under more complex tasks. The fixation count, a metric of cognitive processing, identified areas of pronounced interest influenced by shape, curvature, and texture, with female participants exhibiting distinct fixation patterns emphasizing the role of shape and curvature in evoking emotional responses. Total Fixation Duration, a measure of visual attention, indicated that participants allocated substantial time to examining angular and deeply curved shapes, particularly focusing on elements like bottle necks, slant heights, and angular regions. The study's findings provide designers with insights into consumer preferences for perception of function (appropriateness) feature of product aesthetics, enabling the creation of products that align with both form and function. This approach can empower companies to enhance product aesthetics and gain a competitive advantage.</p>
72.	<p>Unravelling the mechanism of polarization transfer from spin-1/2 to spin-1 system in solids E Nehra, MK Pandey - Physical Chemistry Chemical Physics, 2024</p> <p>Abstract: An analytic theory based on the concept of “effective-fields” is proposed to explain the mechanism of polarization transfer from spin $I = 1/2$ to spin $S = 1$ in non-rotating (static) solids. Employing an isolated two-spin model system, the matching conditions responsible for polarization transfer in cross-polarization (CP) experiments are identified and described in terms of the single-transition operators. In contrast to other existing treatments, the polarization transfer among spins is quantified through analytic expressions highlighting the individual contributions emerging from all plausible CP matching conditions. The interplay between the CP matching conditions observed in experiments is outlined in both isotropic and anisotropic systems and verified through comparison between simulations based on analytic and exact numerical methods. The predictions emerging from the analytic theory are verified over a wide range of experimentally relevant parameters and could be beneficial in the optimization of the CP experiments.</p>
73.	<p>Waste heat recovery from the biomass engine for effective power generation using a new array-based system R Goswami, S Ganguly, R Das - Sustainable Energy Technologies and Assessments, 2024</p> <p>Abstract: Thermoelectric generator -thermosyphon-based heat recovery system for harvesting the heat from the high temperature sources is a well-known technology for power generation. However, various thermal resistances (a total of nine) are involved in the thermosyphon-based between the heat sources and which generate irreversibility that ultimately reduces its performance. In this work, a new design of i.e. TEG-array-based is proposed for effective power generation even at low temperatures of sustainable heat source by minimizing the thermal resistances. This TEG-array-based is driven by a salt gradient thermal storage device (SGTSD) which is used for efficiently recovering and storing of sustainable waste heat generated from a biomass(renewable energy)-based engine-generator. The proposed system is experimentally studied to analyse the temperature variations in characteristics of sustainable waste heat temperature, and performance features of in terms of obtained electrical parameters, output power and conversion efficiency. The experimental results showed that the maximum open circuit voltage, output power and conversion efficiency of are obtained as respectively. With this proposed system, seven thermal</p>

resistances (out of total nine) are totally eliminated while the others two are lowered that leads to effectively transfer the energy from sustainable heat source to via minor equivalent thermal resistance of The proposed system is found to be capable of charging a heavy-duty battery for real life applications.



Disclaimer: This publication digest may not contain all the papers published. Library has compiled the publication data as per the alerts received from Scopus and Google Scholar for the affiliation “Indian Institute of Technology Ropar” for the month of January, 2024. The author(s) are requested to share their missing paper(s) details if any, for the inclusion in the next publication digest.